

# FINITE ELEMENT ANALYSIS OF COMPATIBILITY METRICS IN FRONTAL COLLISIONS

## Pradeep Mohan

FHWA/NHTSA National Crash Analysis Center,  
The George Washington University,

## David L. Smith

National Highway Traffic Safety Administration (NHTSA)  
United States of America  
Paper Number 07-0188

## ABSTRACT

Several numeric measures have been proposed to assess crash compatibility between two vehicles. The measures under investigation in this study are the Average Height of Force 400 (AHOF400) and the Crush-Work Stiffness 400 (Kw400), both measured in 35 mph full-frontal rigid load cell barrier tests. AHOF400 is a measure of the vertical centroid of forces exerted on the barrier surface for the first 400 mm of crush. Kw400 is a measure of the work required to crush 400 mm of a vehicle's front end.

Several studies in the past have concluded that there are large inherent errors in the AHOF measure. One of the main factors influencing the error in this measure is the size of the load cell on the barrier face. In this study, different barrier concepts are examined which can reduce or eliminate the dependency of AHOF400 on load cell size. A finite element analysis was used as a basis to recommend a barrier design that can accurately measure AHOF400. In addition, the influence of impact speed and vehicle mass on AHOF400 and Kw400 are discussed.

Due to the errors associated with the height of force measurement, the relationship between occupant injury measures and height of force matching in the light vehicle crash data is not well understood. The barrier proposed in this study, which eliminates the error in the AHOF400 measure, will enable us to better understand the effects of height of force matching in the vehicle fleet.

## INTRODUCTION

In recent years, the trend of growing sales of sport utility vehicles (SUVs) and pick-up trucks, generally referred to as Light Trucks and Vans (LTVs), has led to renewed public attention on the crash compatibility issue. This issue has been discussed by several researchers [1-5]. It has been generally agreed that the crash incompatibility between vehicles be attributed to three vehicle factors: (1) mass

incompatibility (2) stiffness incompatibility and (3) geometry incompatibility.

Mass has a strong influence on the level of compatibility of two vehicles involved in a collision. Due to the fact that the change in momentum of each body involved in a collision is equal, the lighter body experiences a higher change in velocity during the collision [6]. However, in this study, mass was treated as a condition of the crash and not as a design variable.

Stiffness compatibility is a complex issue. Several studies have tried to establish a relationship between mass and stiffness [7-9]. These studies have shown a weak correlation between mass and stiffness, thus indicating that mass and stiffness are independent vehicle characteristics. Achieving stiffness compatibility is a challenging goal, given the possible goal conflict between self and partner protection, especially for the heavier vehicles.

Front-end geometry influences the potential for structural interaction in a car-to-car collision. Improving the geometric compatibility is the most feasible first step to improve vehicle crash compatibility. Vehicle geometry can be varied, within limits, independent of vehicle mass [6].

This study provides an engineering analysis for quantifying stiffness and geometry metrics to assess vehicle compatibility in frontal crashes.

## COMPATIBILITY METRICS

Worldwide research is ongoing to quantify a vehicle's structure through a dynamic performance test and associated metrics to balance the aggressivity/vulnerability across the vehicle fleet [10]. The metrics under consideration in this study are the Crush-Work Stiffness 400 (Kw400) and Average Height of Force 400 (AHOF400), both measured in 35 mph full-frontal rigid load cell barrier tests.

## Stiffness Metric

The stiffness metric referred to as Crush-Work Stiffness ( $K_{w400}$ ) is derived from equating ideal spring energy to the work of crushing the vehicle front end [9].  $K_{w400}$  is the symbol for a metric that comes from the integral of the area under the force-displacement curve evaluated between 25 to 400 mm of front-end crush as illustrated in the first equation below.

$$\int_{25}^{400} F dx = \frac{1}{2} K_{w400} [(400)^2 - (25)^2]$$

$$F(400 - 25) = \frac{1}{2} K_{w400} [(400)^2 - (25)^2]$$

$$K_{w400} = \frac{2F}{425}$$

Here,  $F$  is the average of the total force exerted on the rigid barrier wall between 25 and 400 mm of vehicle crush. Thus,  $K_{w400}$  is directly proportional to amount of energy it takes to crush the vehicle front end. A low  $K_{w400}$  is a soft vehicle, and high  $K_{w400}$  is a stiff vehicle.

The first 25 mm of crush is ignored intentionally in the  $K_{w400}$  calculation. This is due to several factors such as soft materials in the initial crush, the noise and the cross-talk in the measured data and the distortions caused by the band-pass filter that is traditionally used in processing crash test data. Therefore the calculations are not begun until the vehicle crush reaches 25 mm. The maximum crush is limited to 400 mm to isolate the high inertial forces on the load cell wall due to engine contact.

Force was obtained from the load cell array placed on the rigid wall for research purposes during the US New Car Assessment Program (USNCAP) tests. Displacement was obtained from double integrating the acceleration measured from the accelerometers placed at the front seat cross-members. Both force and acceleration were sampled at 10 KHz. But, once force is cross-plotted vs. displacement, the  $F$ - $d$  curve is no longer at a fixed step size as displacement is a non-linear function of time. The force-displacement data were re-sampled with a fixed step size in displacement before computing average force  $F$  to avoid errors in the  $K_{w400}$  measure.

To illustrate the  $K_{w400}$  calculation, consider two NCAP tests as shown in figure 1. Test 5303 is the NCAP test of an SUV and test 5326 is the NCAP test

of a compact car. The force-displacement curves for the two tests are shown in Figure 1.  $K_{w400}$  calculated for these two vehicles using the above method is shown in Figure 2.

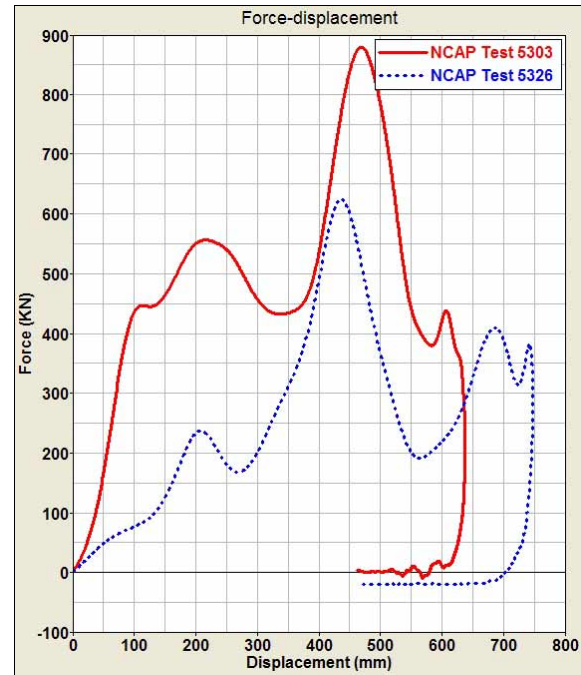


Figure 1. Force-displacement curves for an SUV and a compact car.

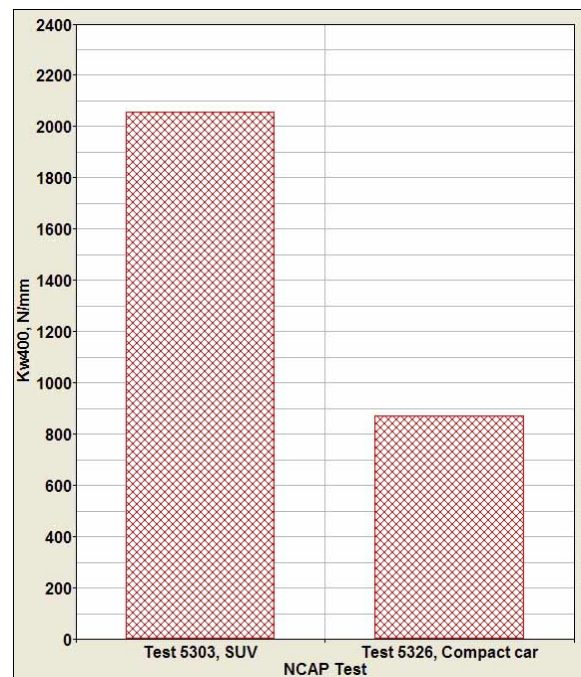
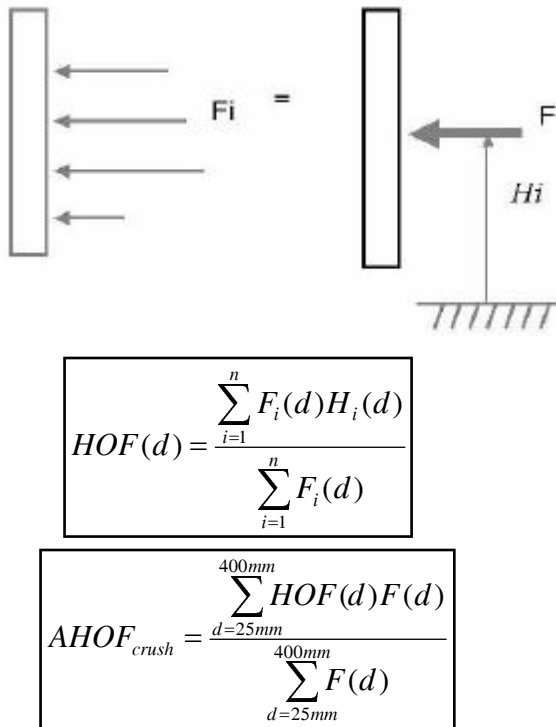


Figure 2.  $K_{w400}$  for an SUV and a compact car.

## Geometry Metric

The geometry metric referred to as the AHOF400 is derived from the height at which the vehicle imparts force to the rigid wall. When a vehicle hits the load cell barrier in a full frontal impact, the individual forces measured on the array of load cells are used to calculate the Height of Force (HOF). Each of the load cell forces,  $F$ , from the load cell wall at a given time are multiplied by their respective height from the ground, summed, and then divided by the sum of all the forces as illustrated in Figure 3. In the HOF equation, “ $n$ ” represents the number of load cells and “ $d$ ” represents the vehicle crush. The AHOF400 is the weighted average of the HOF values during the first 25 to 400 mm of vehicle crush as illustrated in the below equation. The first 25 mm of crush is ignored intentionally in the AHOF400 calculation for the same reasons explained earlier.



**Figure 3. Height of force calculation.**

Several studies in the past have concluded that there are large inherent errors in the AHOF measure [11-14]. In the current frontal USNCAP testing, the full-width rigid barrier is instrumented with single-axis load cells. The HOF measured in these tests has a large source of error.

For example, consider a force,  $F_x$ , applied at the lower most point on the surface of the single-axis

load cell of size  $d$  as shown in Figure 4. As illustrated in the Figure, the force measured by the single-axis load cell is assumed to be at its center irrespective of the actual position of the applied force. Thus, using single-axis load cells, the error in height of force measurement could be as high as  $\frac{1}{2}$  the load cell size. One of the main factors influencing the error in height of force measurement using single-axis load cells is the size of the load cell on the barrier face [15].

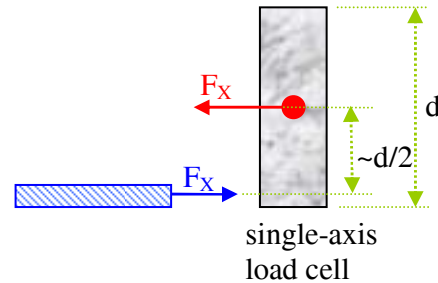


**Figure 4. Measurement error in single-axis load cells.**

## RESULTS AND DISCUSSION

Finite element simulations using LS-DYNA were conducted to evaluate the error content in the AHOF400 computed from rigid wall data and also robustness of the AHOF400 and Kw400 metrics. Three different vehicle Finite Element (FE) models (1996 Dodge Neon, 2003 Ford Explorer and 1999 Dodge Caravan) shown in Figure 5 were used in this study. These vehicle models were chosen so as to represent different class of vehicles in the current US vehicle fleet. These models have been previously validated to a full frontal USNCAP test and the validation reports are available for download from the NCAC website.

<http://www.ncac.gwu.edu/vml/models.html>



**Figure 5. Vehicle FE models (Neon, Explorer and Caravan).**

As discussed above, the accuracy of the AHOF400 is dependent on the size of the axial load cells used to measure the HOF. In order to avoid this problem in simulation studies, the true AHOF400 was computed for the three vehicle models using a single load cell on the rigid wall as illustrated in Figure 6. The load cell used here measured force in the impact direction and also the moment about the y-axis as a function of the applied force. By using this load cell it was possible to locate the exact location of force on the vertical axis, thus leading to a precise estimate of the AHOF400.

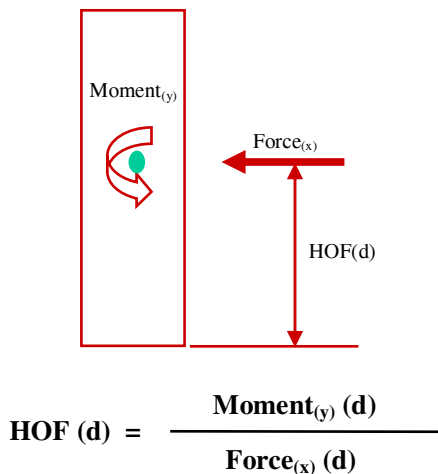


**Figure 6. True/Actual AHOF400 calculation.**

True AHOF400 computed for the three vehicle models is shown in Figure 7. A current industry proposal for a voluntary matching zone for geometrically compatible vehicles is the Part 581 low speed bumper zone that spans from 16 inches (406.4 mm) to 20 inches (508 mm) above the ground [16]. This zone could provide for common interaction of vehicles and needs special attention for the collection of height data and the matching of height metrics like AHOF400.

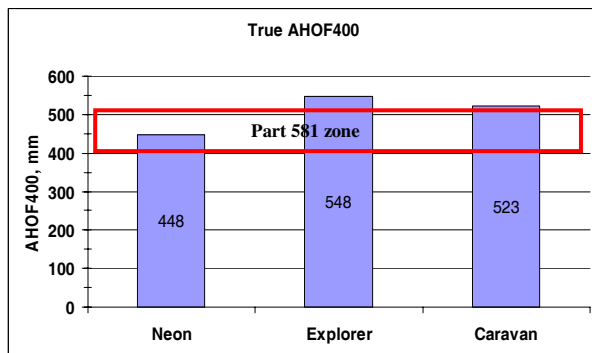


**Figure 7. True/Actual AHOF400 comparison.**

## METRICS ROBUSTNESS STUDY

Real world crashes occur at a wide range of impact speeds, vehicle masses and depend on several other variables. No two real world crashes are identical. A metric chosen to define a compatible vehicle should not heavily depend on these variables under nominal conditions. Several simulation studies were conducted to evaluate the influence of impact speed and vehicle mass on AHOF400 and Kw400.

### Influence of Impact Speed on AHOF400

In addition to the USNCAP simulation, two additional finite element simulations were conducted for the three vehicle types at 30 and 40 mph. The vehicle components, predominantly steel structures, exhibit strain rate effects. This means, the stress at which yield occurs is dependent on the rate of deformation. These rate effects have been included in the vehicle models to ensure accurate prediction of the crash response at different impact speeds [17, 18]. True AHOF400 was computed for each of these simulations using the method explained earlier. The variation in AHOF400 for the three vehicles at three different speeds is shown in Figure 8. The minimum and maximum AHOF400 was 442 mm and 453 mm respectively for the Dodge Neon. Minute variations in AHOF400 were observed for the other vehicle types as well at the different impact speeds. Based on the simulation results, it was concluded that impact speed has negligible effect on this measure.

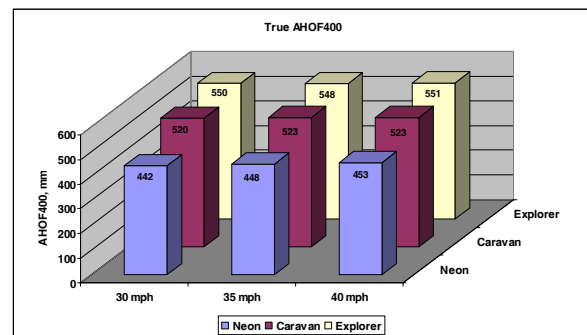


**Figure 8. Influence of impact velocity on AHOF400.**

### Influence of Vehicle Mass on AHOF400

The next step in this study was to understand the influence of vehicle mass on AHOF400. The three vehicle models were massed incrementally to different level of occupancy starting from the unloaded vehicle weight. These masses were rigidly attached to the vehicle at the designated seating positions. Table 1 shows the mass increments

considered for the Dodge Neon, which were incremented above the unloaded design weight (UDW). Similar mass increments were considered for the Ford Explorer and Dodge Caravan. With each mass increment there will be minor change in ride heights of the vehicle. The ride height difference was not considered in this study as there was no accurate way of determining the effect of mass on ride height of these vehicles, especially using crash based finite element vehicle models. Simulations were conducted for these five mass increments using USNCAP test conditions. The simulation results showed that mass has negligible influence on AHOF400. The force-deflection curves were identical for the first 400 mm of crush in each of these simulations. Based on this study, it was concluded that AHOF400 is a function of the vehicle design. Assuming the change in ride height is negligible, added vehicle mass and speed have negligible effect on this metric.

**Table 1.**  
Mass increments for Dodge Neon

Dodge Neon	UDW (kg)	Number of occupants	Total Mass (kg)
	1155	1	1231
2		1307	
3		1383	
4		1459	
5		1535	

**Influence of Impact Speed on Kw400**

The Kw400 for the three vehicle models was calculated using the method explained earlier and is shown in Figure 9, note that these results are for the 35 mph impact speed.

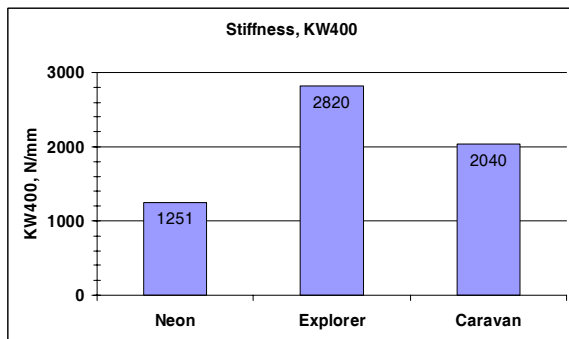


**Figure 9. Kw400 comparison.**

Finite Element simulations were conducted at 30, 35 and 40 mph to determine the influence of impact speed on Kw400 metric. The variation of Kw400 for the three vehicle models at different impact speeds is shown in Figure 10. The maximum variation of

Kw400 with impact speed was 22% for the Dodge Neon, 32.5% for the Dodge Caravan and 13.5% for the Ford Explorer.

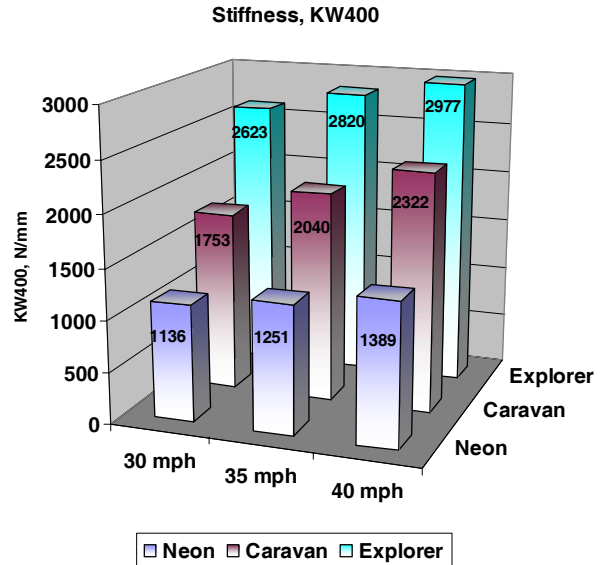


**Figure 10. Influence of impact velocity on Kw400.**

To further examine this variation, consider the force-displacement curves for the Ford Explorer and Dodge Caravan shown in Figures 11 and 12. The F-d curves for the Ford Explorer showed similar response until the vehicle experienced about 350 mm of crush at the three impact speeds. The overall vehicle crush reached only 400 mm at 30 mph impact speed. At 35 mph impact, the kinetic energy increased to 1.36 times to that of the 30 mph impact. At 40 mph the increase in kinetic energy was 1.77 times. To satisfy the principle of conservation of energy, the vehicle had to absorb more energy at 35 and 40 mph respectively. This is accomplished by reaching higher crush levels, thus increasing the energy absorbed by the vehicle at higher speeds. An interesting thing to note in these Figures is that the F-d curves for the Dodge Caravan start deviating earlier, at about 150 mm of crush, when compared to the Ford Explorer. The overall crush in the Dodge Caravan reached 535 mm at 30 mph. Due to higher kinetic energy at 35 and 40 mph the Dodge Caravan reached crush levels of 630 mm and 730 mm, respectively. The Dodge Caravan is a unibody construction and has multiple load paths which highly influence the force-displacement characteristics at different impact speeds. The Ford Explorer, on the other hand, is body-on-frame type construction. Since the frame rails form the primary load path in this type of construction, the F-d curves showed little variation up to 350 mm of crush. Based on the above observations, it was concluded that the

vehicle design and impact speed has a strong influence on Kw400.

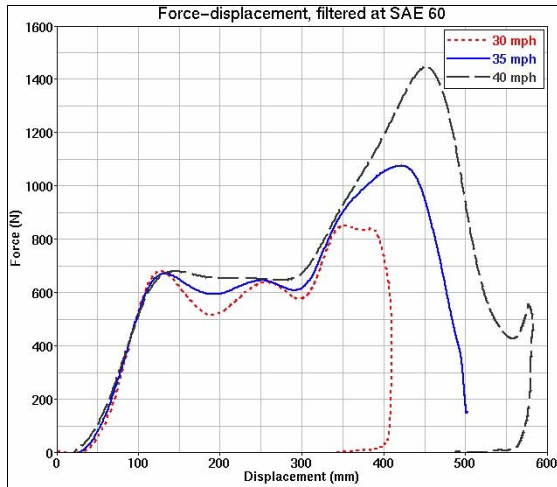


**Figure 11. FE force-displacement curves for Ford Explorer at three different impact velocities.**

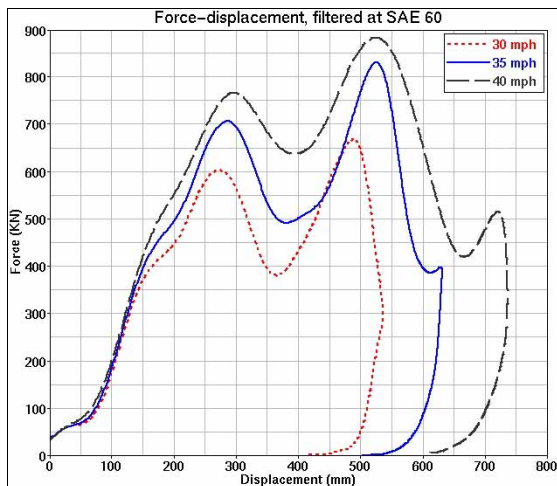


**Figure 12. FE force-displacement curves for Dodge Caravan at three different impact velocities.**

At higher closing speeds, the Kw400 for each of the vehicle models increased. This shows that the work done to reach the 400 mm crush level increased as the impact speed increased. In a two-vehicle crash, the relative size of the metrics is critical. Thus, the ratio of the stiffness metrics should remain constant as the crash speed is varied in order for this metric to be useful. Under this consideration, the Explorer/Neon stiffness ratio is seen to be 2.31, 2.25, and 2.14 as the test speed is varied from 30 to 40 mph. Similarly, the Caravan/Neon stiffness ratio is seen to be 1.54, 1.63, and 1.67 as the speed is

increased. These ratios show good consistency across the range of energy conditions studied and thus indicate good usefulness.

### Influence of Vehicle Mass on Kw400

In order to determine the influence of vehicle mass on Kw400, the vehicle models were massed incrementally to different levels of occupancy starting from the unloaded vehicle weight. Again, these masses were added to the vehicle so as to represent the occupied seating position. Table 2 summarizes the mass increments considered for the Dodge Neon.

**Table 2.  
Kw400 for Dodge Neon at Different Mass Increments**

Dodge Neon	UDW (kg)	Number of occupants	Total Mass (kg)	Kw400 (N/mm)
	1155	1	1231	1261.2
		2	1307	1260.1
		3	1383	1249.2
		4	1459	1247.9
		5	1535	1250.9

The total mass rose from 1231 Kg with one occupant to 1535 Kg with five, a 25% increase. The force-displacement curves for these simulations are shown in Figure 13. The change in kinetic energy with different mass increments showed no noticeable difference in the force-displacement curves in the Kw400 evaluation region of 400 mm vehicle crush. Overall vehicle crush slightly increased with increased kinetic energy. For each of these cases the value of Kw400 was computed according to the method described earlier. The lowest value computed was 1247.9 N/mm and the highest was 1261.2. The maximum variation was about 1%.

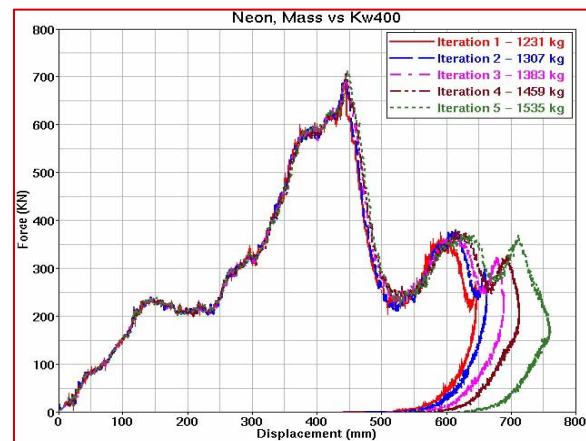


**Figure 13. FE force-displacement curves for Dodge Neon at different mass increments.**

A similar study of added mass was conducted for the Ford Explorer. Table 3 summarizes the mass increments considered. The mass increase was about 15%, the total mass increased from 2116 Kg with one occupant to 2420 Kg with five. The maximum variation in the Kw400 measure was about 1%. This is a negligible variation in computed values.

**Table 3.**  
**Kw400 for Ford Explorer at Different Mass Increments**

	UDW (kg)	Number of occupants	Total Mass (kg)	Kw400 (N/mm)
Ford Explorer	2040	1	2116	2828.2
		2	2192	2827.8
		3	2268	2820.7
		4	2344	2812.9
		5	2420	2800.1

From this study, the simulation results suggested that Kw400 is predominantly a function of vehicle design. Added vehicle mass under nominal conditions was shown to have no influence on this metric. Kw400 does show some dependence on impact speed, but this effect seems to be similar for all vehicles so stiffness ratios remain fairly constant. This needs to be further investigated.

### BARRIER DESIGN

The next step in this study was to determine a rigid barrier design that provides the data required to accurately compute the height of force and stiffness data needed. Full width rigid load cell barrier concepts were proposed based on a load cell resolution study [15]. Since the part 581 zone spans about 100 mm vertically, it was critical to locate the exact HOF for fleet matching as proposed by the Alliance voluntary agreement. [16]. For an assumed 10% error allowance, only  $\pm 10$  mm error would be allowed for this zone. However, the load cell resolution study showed that the error in AHOF400 measurement was greater than 10mm unless 62.5 mm single-axis square load cells were used to instrument the barrier. Further, this did not eliminate the error altogether. Earlier in the paper (figure 6) the need for an added moment channel (My) to accurately measure HOF was discussed. To this end, 4 barrier concepts and variants of those with multi-axis load cells are considered for the cost analysis. The following criteria were considered in proposing these concepts:

- Barrier length and width to fit all previous frontal NCAP vehicles

- Possibility of calculating International Research Harmonization Activity (IHRA) recommended compatibility metrics [19]
- Ability to accurately compute AHOF400 and analyze forces distribution in the Part 581 zone.

The Concept 1 barrier was instrumented with five rows and nine columns of 250x250 mm load cells (Fx and My) and is shown in Figure 14. A ground clearance of 80 mm was chosen for the barrier such that the Part 581 zone lies in the center of the 2nd row of load cells. This barrier is similar to the barrier used in conjunction with USNCAP except that multi-axis load cells are used instead of single-axis load cells. An additional row and column have been added to accommodate the larger SUVs and pickups anticipated in future USNCAP tests.

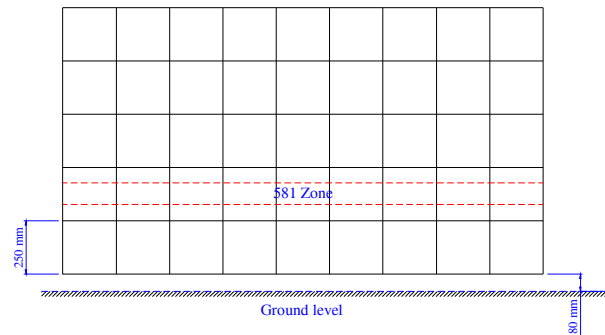


**Figure 14. Barrier concept 1.**

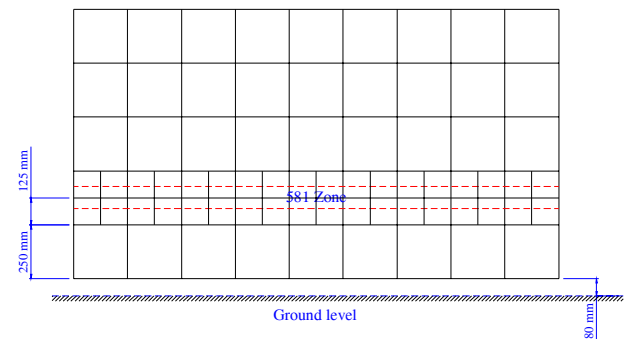


**Figure 15. Barrier concept 2.**

The Concept 2 barrier was instrumented with 250x250 mm load cells (Fx and My) throughout except for the 2nd & 3rd rows. This area is defined as the “Common Interaction Zone” among European researchers. The 2nd and 3rd rows are instrumented with 125 mm load cells (Fx only), which are placed with respect to the Part 581 zone according to the positions for the IHRA barrier and would allow limited comparison of data internationally in this region. This concept is shown in Figure 15. Concept

2a is similar to concept 2. The only difference is that, multi-axis load cells are used to instrument the rigid barrier in the common interaction zone instead of single-axis load cells.

The Concept 3 barrier is similar to Concept 2 barrier. It is instrumented with 250x250 mm load cells (Fx and My) throughout except for the 2nd & 3rd row. The 2nd and 3rd rows are instrumented with 100 mm load cells (Fx only) to give clear coverage to the Part 581 zone. The ground clearance had to be adjusted to 56.4 mm such that the 3<sup>rd</sup> row of load cells overlaps the Part 581 zone. This concept is shown in Figure 16. Concept 3a is similar to concept 3. The only difference is that, multi-axis load cells are used throughout to instrument the rigid barrier instead of single-axis load cells.

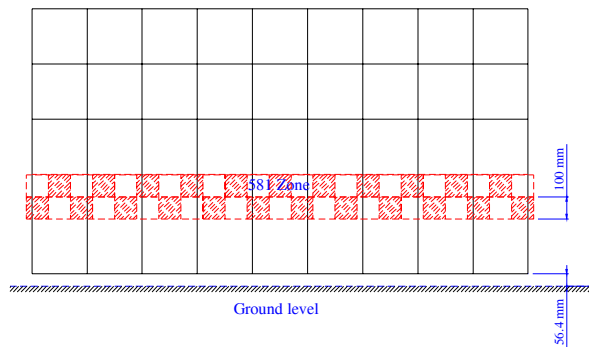


**Figure 16. Barrier concept 3.**

The Concept 4 barrier is instrumented with 125x125 mm load cells (Fx only) throughout and is shown in Figure 17. The load cells in this concept are the same size as those used by IHRA and other international bodies, though the load cells in those barriers are covered with 2 layers of deformable honeycomb. This configuration would allow the best possible sharing of data between NHTSA and the international test and evaluation community. Concept 4a is similar to concept 4. The only difference is that, multi-axis load cells (Fx and My) are used to instrument the rigid barrier instead of single-axis load cells.

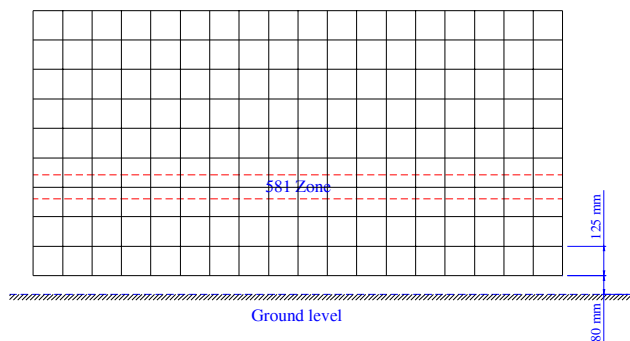


**Figure 17. Barrier concept 4.**

### Barrier Selection Criteria

Several variants of these proposed concept barriers with single-axis and multi-axis load cells were considered in the cost/benefit study. The barrier selection and recommendation was based on the following criteria:

- Accuracy in measuring AHOF400
- Possibility of measuring HNT/VNT (horizontal and vertical structural distributions) as proposed by IHRA [19]
- Initial cost of the barrier
- Cost of test data collection per test
- Cost of quality control per test

While a 9x18 load cell array measuring axial force only does not have the accuracy needed for AHOF400 metrics [15], it is nevertheless included in several cases for cost comparison purposes. Appendix A summarizes the cost/benefit study for different barrier concepts and its variants.

Budgetary quotes were obtained from 4 load cell manufacturers active in the crash testing field. The current cost of test data collection per channel is \$23 and the cost of quality control per channel is \$4. These costs are the same for all barriers, but the number of data channels makes a great difference to overall costs.

Concept barrier 1 is sufficient and necessary to accurately measure AHOF400. The initial cost to purchase this barrier is comparable to some of the other concepts. Further, the cost/test with this barrier concept is lower compared to other concepts because it has fewer data channels. However, this barrier was not recommended as it does not provide an opportunity to gather data required to compute IHRA recommended compatibility metrics.

Barrier concept 4a was recommended based on the findings of this study for two reasons. First, this barrier can accurately measure AHOF400 compared to the IHRA barrier, which could not. Second, if NHTSA decides to harmonize the compatibility tests with IHRA and international stakeholders, a deformable layer of honeycomb can be added to this barrier in order to measure the distribution type compatibility metrics defined by IHRA. The only shortcoming of this barrier is the added data channels required in each test. This adds the cost of test data collection and quality control to the cost of each test.

Further, these additional data channels add to the initial cost of the barrier, though the initial cost estimates varied widely from comparable to other designs to much more expensive. Subsequent conversations with load cell manufacturers have indicated that several testing facilities are interested in this barrier concept, some are purchasing and some are awaiting NHTSA's purchase decision.

## CONCLUSIONS

AHOF400 and Kw400 were analyzed as metrics that could capture the key vehicle compatibility characteristics of height of force and energy absorption in the frontal compartment, respectively. AHOF400 ensures that the vehicle structures engage properly, reducing under ride and override. Kw400 ensures that the crash energy is properly shared between the impacting vehicles.

The dependence of AHOF400 and Kw400 metrics on impact speed and vehicle mass was investigated through computer simulations. Three different impact speeds (30, 35 and 40 mph) were considered. Five different mass increments were evaluated at the NCAP test condition. The results of these simulations showed that vehicle mass and impact speed under nominal conditions have no influence on AHOF400. Although vehicle mass showed no influence on Kw400, it did show some dependence on impact speed. Nevertheless, stiffness ratios show good constancy across a wide range of crash energy and should be investigated further.

Several finite element studies were performed to lay a basis for improved barrier design and a best concept to meet multiple criteria was selected. The load cells that are used to instrument the rigid barrier should measure a minimum of two channels (X-force and Y-moment as a function of the applied force) to accurately locate the height of force. The new barrier proposed in this study is expected to create better source data for accurate height of force estimates.

## REFERENCES

[1] Gabler, H. C. and Hollowell, W. T., "NHTSA's Vehicle Aggressivity and Compatibility Research Program", Proceedings of the Sixteenth International Enhanced Safety of Vehicle Conference, Paper No. 98-S3-O-01, Windsor, Canada (1998)

[2] Gabler, H. C. and Hollowell W. T., "The Aggressivity of Light Trucks and Vans in Traffic Crashes", Society of Automotive Engineers Paper No. 980908, February 1998

[3] Summers, S., Hollowell, W.T., Prasad, A., "NHTSA's Research Program for Vehicle Compatibility", 18th International Conference on the Enhanced Safety of Vehicles, Paper 307, May 2003.

[4] Verma, M.K., Lavelle J., Lange R.C., "Perspectives on Vehicle Crash Compatibility and Relationship to Other Safety Criteria", 18th International Conference on the Enhanced Safety of Vehicles, Paper 412, May 2003.

[5] Reilly, P.O., "Status Report of IHRA Compatibility and Frontal Impact Working Group", 18th International Conference on the Enhanced Safety of Vehicles, Paper 402, May 2003.

[6] Thomas, G., Zobel, R., Schwarz, T., "Required Measures to Improve the Structural Interaction Potential of Passenger Cars", Society of Automotive Engineers, Paper No. 2005-01-1351, March 2005.

[7] Nusholtz, G., Rabbiolo, G., and Shi, Y., "Estimation of the Effects of Vehicle Size and Mass on Crash-Injury Outcome through Parameterized Probability Manifolds", Society of Automotive Engineers, Paper no 2003-01-0905, March 2003.

[8] Mizuno, K., Kajzer, J., "Compatibility Problems in Frontal, Side, Single Car Collisions and Car-to-Pedestrian Accident in Japan", Accident Analysis and Prevention, Pages 381-391, 1998.

[9] Nusholtz, G., et al "Vehicle Mass, Stiffness and their Relationship", Twentieth International Technical Conference on the Enhanced Safety of Vehicles, Paper No. 05-0413, 2005.

[10] Mizuno, K., Tateishi, K., Ezaka, Y., "Test Procedures to Evaluate Vehicle Compatibility", Seventeenth International Technical Conference on the Enhanced Safety of Vehicles, Paper No. 127, Amsterdam, 2001.

[11] Verma, M. K., Nagappala, R., et al "Significant Factors in Height of Force Measurements for Vehicle Collision Compatibility", Society of Automotive Engineers, Paper No. 2004-01-1165, March 2004.

[12] Jerinsky, M., Hollowell, T., "NHTSA's Review of Vehicle Compatibility Performance Metric Through Computer

- Simulation”, ASME International Mechanical Engineering Congress and Exposition, Paper Number IMECE2003-44045, Washington, D.C., 2003.
- [13] Takizawa, S., Sugimoto, T., Suzuki, K., “A Study of Compatibility Test Procedure in Frontal Impact”, 18th ESV, Paper Number 437, Nagoya, 2002.
- [14] Jerinsky, M., Hollowell, T., “NHTSA’s Review of High-Resolution Load Cell Wall’s Role in Designing for Compatibility”, 18th ESV, Paper Number 393, Nagoya, 2003.
- [15] Mohan, P., Marzougui, D., Kan, C.D., “Modified Approach to Accurately Measure Height of Force (HOF)”, Society of Automotive Engineers, Paper Number 2007-01-1182, April 2007.
- [16] Barbat, S., “Status of Enhanced Front-to-Front Vehicle Compatibility Technical Working Group Research and Commitments”, 19<sup>th</sup> ESV, Paper Number 05-0463, Washington D.C, 2005.
- [17] Simunovic, S., Nukala, V., et al., “Modeling of Strain Rate Effects in Automotive Impact”, Society of Automotive Engineers, Paper No. 2003-01-1383, March 2003.
- [18] Xu, K., Wong, C., et al., “High Strain Rate Constitutive Model for High Strength Steels”, Society of Automotive Engineers, Paper No. 2003-01-0260, March 2003.
- [19] O’Reilly, P., “Status Report of IHRA Compatibility and Frontal Impact Working Group,” 19th ESV, Paper Number 05-0365, Washington D.C, 2005.

APPENDIX A – LOAD CELL BARRIER COST/BENEFIT STUDY

	Crash wall description	Accuracy in measuring AHOF400	Ability to calculate HNT/VNT	Budgetary quotes from load cell manufacturer's				Cost of data collection per test	Number of channels for QC	Cost of QC/test
				1	2	3	4	\$23/channel		\$4/channel
Concept 1	250 mm LC (Fx & My)	Highly accurate	Not possible	\$548K	\$234K	\$316K	\$322K	\$2,070	90	\$360
Concept 2	250 mm LC (Fx & My), 125 mm LC (Fx)	Error due to single-axis LC in rows 2 and 3. This error could be as high as 1/2 the loadcell size (62.5 mm)	Can be computed based on IHRA's definition	\$622K	\$241K	\$443K	\$330K	\$2,484	108	\$432
Concept 2a	250 mm LC (Fx & My), 125 mm LC (Fx & My)	Highly accurate	Can be computed based on IHRA's definition	\$664K	\$324K	\$458K	\$347K	\$3,312	144	\$576
Concept 3	250 mm LC (Fx & My), 100 mm LC (Fx)	Error due to single-axis LC in rows 2 and 3. This error could be as high as 1/2 the loadcell size (50 mm)	Not possible	\$628K	\$256K	\$472K	\$356K	\$2,714	118	\$472
Concept 3a	250 mm LC (Fx & My), 100 mm LC (Fx & My)	Highly accurate	Not possible	\$680K	\$362K	\$491K	\$374K	\$3,772	164	\$656
Concept 4	125 mm LC (Fx)	Error due to single-axis LC. This error could be as high as 1/2 the loadcell size (62.5 mm)	Can be computed based on IHRA's definition	\$286K	\$243K	\$863K	\$310K	\$3,726	162	\$648
Concept 4a	125 mm LC (Fx & My)	Highly accurate	Can be computed based on IHRA's definition	\$437K	\$616K	\$932K	\$374K	\$7,452	324	\$1,296